JOURNAL OF MATERIALS SCIENCE 30 (1995) 720-723

A stabilization mechanism of M_2O_3*c*-type rare earth tetragonal stabilized ZrO_2 via co-decomposition

G. PRETORIUS
Department of Chemistry, University of Pretoria, 0002, South Africa

Evidence was obtained that *c*-type rare earth M_2O_3 stabilized ZrO_2 in the tetragonal phase via oxygen coordination between the M_2O_3 molecule and the ZrO_2 unit cell. The ratio for 100% stabilization was calculated to be 2.7 mol% M_2O_3 stabilizer. This was experimentally proved by using the co-decomposition process to obtain 100% tetragonal stabilization efficiency. It has also been established that stabilization is dependant upon the average Zr–O bond length of 226 pm as a parameter and not necessarily of an exact radius varying between 206 pm and 246 pm.

1. Introduction

Tetragonal ZrO_2 is widely used in the manufacturing of PSZ [1] and TZP [2–5] ceramics. One of the methods used to stabilize ZrO_2 in a tetragonal phase is via a chemical co-precipitate intermediate [6], prior to calcination. Misunderstanding prevails in this area since many researchers believe that the stabilization efficiency is due to the co-precipitate intermediate and neglect the calcination (decomposition) reaction. Recently, tetragonal ZrO_2, was prepared without any stabilizer and intermediate, which is stable at room temperature [7]. This led the way to the investigation into tetragonal stabilization processes and the mechanism by which tetragonal stabilization occurs.

2. Experimental procedure

2.1. Sample preparation

$Zr(SO_4)_2.xH_2O$ grade 4 (> 99% pure) was obtained from Phalaborwa Mining Company, South Africa. Analytical grade M_2O_3, M = Sb, In, Eu, Ho, Nd, Pr, Ce, Bi was bought from Fluka and $M_2(SO_4)_3.xH_2O$ was prepared via the reaction of M_2O_3 with H_2SO_4.

2.2. Thermogravimetric analysis

A Stanton–Redcroft STA 780 simultaneous thermal analyser was used to obtain thermogravimetric data. Nitrogen was used as a dynamic atmosphere with a flow rate of approximately 20 $cm^3 min^{-1}$. Platinum sample pans were used and temperature calibration was achieved by using ICTA recommended DTA standards.

2.3. X-ray powder diffraction analysis

X-ray powder diffraction patterns were recorded on a Siemens D501 instrument equipped with a monochromator. CuK_α radiation at 25 mA and 30 kV was used.

2.3.1. The derivation of a calibration curve for tetragonal ZrO_2

The first step was to derive a calibration curve to determine the percentage tetragonal phase present in ZrO_2 as a function of the ratio between the tetragonal and monoclinic intensity reflex signals respectively at $2\theta = 30°$ and $2\theta = 28°$ of an X-ray powder diffraction pattern. This was done by mixing different weighed portions of 100% monoclinic ZrO_2 and 100% tetragonal ZrO_2 thoroughly in acetone, drying it, and then recording the X-ray powder diffraction patterns of the mixed powders. The different ratios between the tetragonal and monoclinic reflex signals respectively at $2\theta = 30°$ and $2\theta = 28°$ were calculated and plotted against the % tetragonal phase used in the weighed portion (Fig. 1).

2.3.2. Calculation of the stabilization efficiency

X-ray powder diffraction patterns of the decomposed products, prepared by different processes containing 1–6 wt% Y_2O_3 in each case, were recorded. The ratios between the tetragonal and the monoclinic intensity reflex signals respectively at $2\theta = 30°$ and $2\theta = 28°$ were calculated. These calculated values were used to derive the percentage tetragonal phase from the calibration curve (Fig. 1). The different percentages of the tetragonal phase were then plotted against the wt% Y_2O_3 used to obtain the efficiency curves for the different processes (Fig. 2).

2.3.3. Preparation of yttria stabilized tetragonal ZrO_2 via decomposition of Zr–Y–OH co-precipitate

Concentrated solutions of Zr $(SO_4)_2$ and $Y_2(SO_4)_3$ were prepared and then standardized by taking certain volumes of these solutions, carefully decomposing them at 1100 °C and then weighing the resulting mass

0022–2461

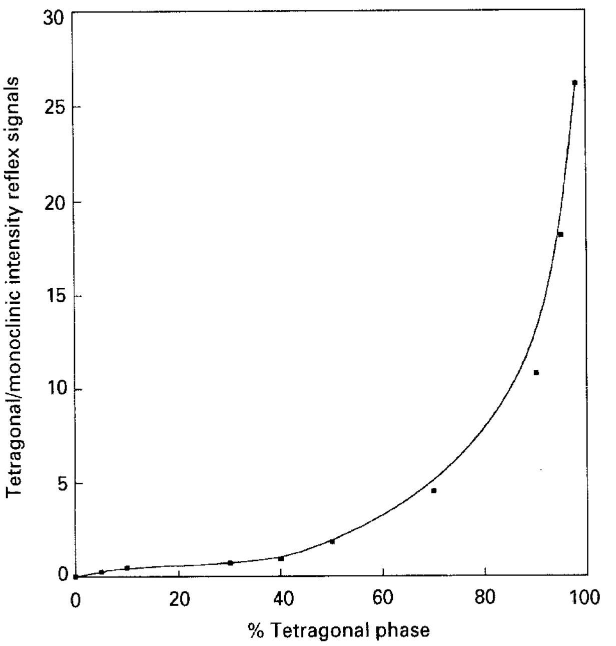

Figure 1 The calibration curve for tetragonal ZrO_2 as a function of the ratio between the tetragonal and monoclinic intensity reflex signals of X-ray powder diffraction patterns, respectively at $2\theta = 30°$ and $2\theta = 28°$.

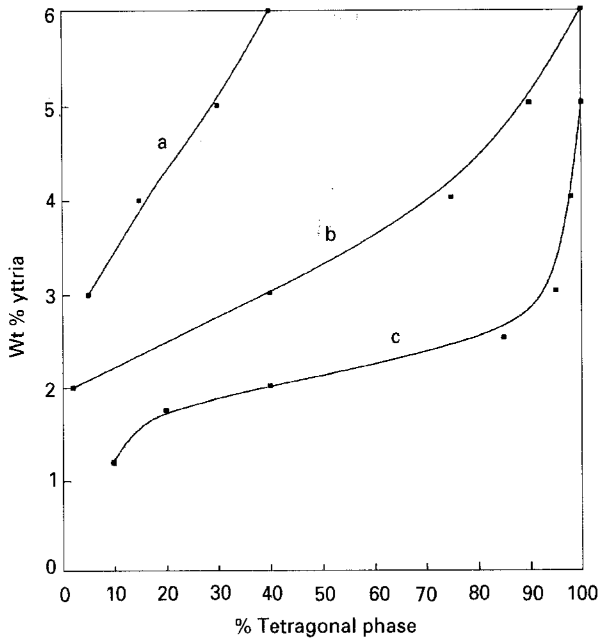

Figure 2 The stabilization efficiency of different decomposition reactions (a) Decomposition of $Zr–Y–SO_4$ at a heating rate of 100 °C h^{-1}. (b) Decomposition of Zr–Y–OH at a heating rate of 100 °C h^{-1}. (c) Decomposition of $Zr–Y–SO_4$ and Zr–Y–OH directly at 1100 °C.

containing ZrO_2 and Y_2O_3 respectively. Mixtures of these two solutions containing between 1–6 wt% Y_2O_3 were co-precipitated by the addition of ammonia to these solutions until the pH was 7. The co-precipitates were then filtered and decomposed at a heating rate of 100 °C h^{-1} up to 1100 °C. Afterwards, the stabilization efficiency of this process was calculated (as described in section 2.3.2.) and the results were plotted in Fig. 2.

2.3.4. Preparation of yttria stabilized tetragonal ZrO_2 via the decomposition of $Zr–Y–SO_4$

The same experimental procedures as in Section 2.3.3 were used except for the addition of ammonia, therefore, no co-precipitated intermediates were present prior to decomposition. Afterwards the stabilization efficiency of this process was calculated and the results were plotted in Fig. 2.

2.3.5. Preparation of yttria stabilized tetragonal ZrO_2 via co-decomposition of $Zr–Y–SO_4$ and Zr–Y–OH respectively

- $Zr–Y–SO_4$: The same experimental procedures as in section 2.3.4 were used except that the decomposition reactions were carried out directly at 1100 °C for 2 h.
- Zr–Y–OH: The same experimental procedures as in section 2.3.3 were used except that the decomposition reactions were carried out directly at 1100 °C for 2 h.

Afterwards the stabilization efficiency of this process was calculated and the results were plotted in Fig. 2.

2.3.6. Preparation of yttria (3 wt%) stabilized tetragonal ZrO_2 via separate precipitation

The same experimental procedures as in section 2.3.2 were used except that the $Zr(SO_4)_2$ and $Y_2(SO_4)_3$ solutions were not mixed prior to the addition of ammonia in both solutions, but thereafter. The same heating rate as in section 2.3.2 (100 °C h^{-1}) was used to decompose this mixture and afterwards the stabilization efficiency was calculated.

2.3.7. Preparation of 2.7 mol% M_2O_3 (M = Sb, In, Y, Eu, Ho, Nd, Pr, Ce, Bi) stabilized tetragonal ZrO_2 via co-decomposition

Concentrated M_2O_3 precursor solutions were prepared and standardized by the decomposition of pipetted volumes of these solutions at 1100 °C and weighing the resulting M_2O_3 powders. Mixtures of a standardized $Zr(SO_4)_2$ solution and a M_2O_3 standardized precursor solution were co-decomposed directly at 1100 °C for 2 h. Afterwards the stabilization efficiency of the different M_2O_3 stabilizers were calculated and are listed in Table I.

3. Results and discussion

Fig. 3 shows the mass–loss curves for the decomposition of $Y_2(SO_4)_3.xH_2O$, $Y(OH)_3.xH_2O$, $Zr(OH)_4.xH_2O$ and $Zr(SO_4)_2.xH_2O$ respectively as a function of time and temperature. These samples were lowered into the furnace of the Stanton–Redcroft STA 780 at 1000 °C. The decomposition of the $Y(OH)_3.xH_2O$ and $Zr(OH)_4.xH_2O$ under these conditions was completed at the same time (just after one

TABLE I Stabilization efficiency of 2.7 mol% *c*-type rare earth M_2O_3

$M_2O_3^a$	r (M-O)^b (pm)	t-ZrO_2 (%)
Sb_2O_3	214	100^c
In_2O_3	218	100^c
Y_2O_3	222	100
Eu_2O_3	227	100
Ho_2O_3	228	100
Nd_2O_3	236	100
Pr_2O_3	237	90
Ce_2O_3	239	5
Bi_2O_3	241	0

^{a}Via decomposition at 1100 °C of M_2O_3 and ZrO_2 precursor solutions.

^{b}Calculated M-O binding length using the values of crystal radii from Shannan [10].

^{c}Via co-decomposition at 900 °C of M_2O_3 and ZrO_2 precursor solutions. At 1100 °C M_2O_3 sublimates leaving monoclinic ZrO_2.

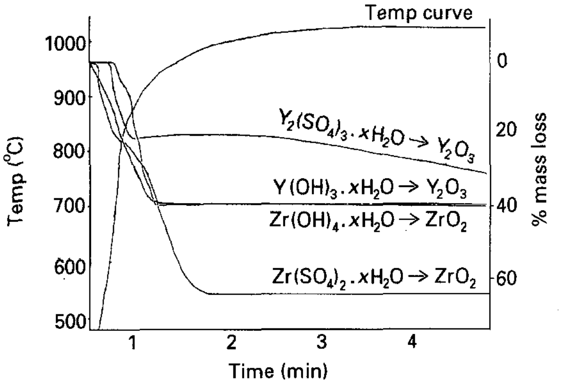

Figure 3 The mass-loss curve of the decomposition of $Y_2(SO_4)_3.xH_2O$, $Y(OH)_3.xH_2O$, $Zr(OH)_4.xH_2O$ and $Zr(SO_4)_2.xH_2O$ in a nitrogen atmosphere as a function of time and temperature.

minute). Therefore we can assume that the decomposition rates for $Y(OH)_3.xH_2O$ and $Zr(OH)_4.xH_2O$ are the same under these conditions. $Zr(SO_4)_2.xH_2O$ reached complete decomposition slightly before two minutes under these conditions while, even at 1000 °C and after five minutes, the $Y_2(SO_4)_3.xH_2O$ was not completely decomposed. We can assume that the decomposition rates of $Y_2(SO_4)_3.xH_2O$ and $Zr(SO_4)_2.xH_2O$ differ under these conditions.

The stabilization efficiency for the different decomposition processes is demonstrated in Fig. 2. The best results (least wt% Y_2O_3 for maximum % tetragonal phase) were obtained by the co-decomposition process. Fig. 3 is a guideline to explain the poor stabilization efficiency of the decomposition of Zr–Y–SO_4 at a heating rate of 100 °C h^{-1} and the relatively good stabilization efficiency of the decomposition of the co-precipitated Zr–Y–OH at the same heating rate. It is also evident that the success for the tetragonal stabilization lies in the simultaneous decomposition of $Y_2(SO_4)_3.xH_2O$ and $Zr(SO_4)_2.xH_2O$. If a solution containing these two salts is heated at 100 °C h^{-1}, the $Zr(SO_4)_2$ starts to decompose to tetragonal ZrO_2. At this stage $Y_2(SO_4)_3$ is mostly undecomposed and there are virtually no Y_2O_3 available to stabilize the tetragonal ZrO_2 in the tetragonal phase. At above 800 °C the newly formed tetragonal ZrO_2 then transformed irreversibly to monoclinic ZrO_2. By the time that the $Y_2(SO_4)_3$ has decomposed to Y_2O_3 it was only able to stabilize approximate 40% of the theoretical possible ZrO_2. Even when the resulting powder is then heated above the phase transformation temperature (1200 °C) of monoclinic ZrO_2 to tetragonal ZrO_2 [8] the nett result remained unchanged.

Further proof that the stabilization efficiency of the decomposition of the Zr–Y–OH co-precipitate is due to the close resemblance of the decomposition rates of $Zr(OH)_4$ and $Y(OH)_3$ and not because of the co-precipitated intermediate, is that the stabilization efficiency of the decomposition of the mixture of separate precipitate of $Y(OH)_3$ (3 wt% Y_2O_3) and Zr $(OH)_4$ at a heating rate of 100 °C h^{-1}, is the same as for the equivalent co-precipitate, namely 40% tetragonal phase.

By co-decomposing the Zr–Y–OH co-precipitate the same stabilization efficiency was obtained as for the co-decomposition of the Zr–Y–SO_4 solution. This proves that the optimum stabilization efficiency is a function of co-decomposition.

The next step is to propose a possible mechanism by which tetragonal stabilization of ZrO_2 occurs and also to predict the theoretical mol% Y_2O_3 necessary to obtain 100% tetragonal stabilization of ZrO_2. A hypothesis is that stabilization occurs when a Y_2O_3 molecule, which is in the matrix of the newly formed 8-coordinated tetragonal ZrO_2 unit cell, coordinates with one of the oxygen atoms of the ZrO_2 unit cell. This coordination prevents the 8-coordinated tetragonal ZrO_2 unit cell to transform to the 7-coordinated monoclinic ZrO_2 unit cell. To calculate the theoretical mol% of Y_2O_3 necessary to stabilize ZrO_2 in the tetragonal phase, one has to start at the coordination number of Y_2O_3 which is 6 for each yttrium atom. Therefore, Y_2O_3 can coordinate with (12-3) 9 other oxygen atoms because it has 3 oxygen atoms of its own. One oxygen atom represents one tetragonal ZrO_2 unit cell. For one tetragonal ZrO_2 unit cell eight oxygen atoms are necessary to coordinate with the Zr-atom. By using the empirical formula, ZrO_2, one 8-coordinated ZrO_2 unit cell needs 4 ZrO_2 molecules to obtain 8 oxygen atoms. Therefore, one Y_2O_3 molecule can stabilize (9 × 4) 36 ZrO_2 molecules in the tetragonal phase. This is a ratio of 1/37 or 2.7 mol% M_2O_3 stabilizer (4.8 wt% Y_2O_3) and is confirmed by Ingel and Lewis [9] when they obtained the optimum density in single crystals of Y_2O_3 stabilized ZrO_2 by using 2.8 mol% Y_2O_3. We can conclude that theoretical 2.7 mol% M_2O_3 molecules with the same crystal structure as Y_2O_3 (*c*-type rare earth) would be able to stabilize ZrO_2 100% in the tetragonal phase. This was put to the test by using the co-decomposition process and the results are listed in Table I.

Tetragonal ZrO_2 has 4 Zr–O bonds with a length of 206 pm and another 4 Zr–O bonds with a length of 246 pm [11]. The average bond length of Zr–O in a tetragonal unit cell is therefore calculated to be

226 pm. All the *c*-type rare earth M_2O_3 that are within 5.4% of 226 pm, stabilized ZrO_2 100% in the tetragonal phase. This not only proves the mechanism of tetragonal stabilization but also the optimum efficiency of the decomposition process. Pr_2O_3 only has 90% stabilization efficiency although it is within 5.4% of 226 pm. The reason probably being that the empirical formula for praseodymium oxide is Pr_6O_{11} and not Pr_2O_3. The poor stabilization efficiency of Ce_2O_3 and Bi_2O_3 is probably because they fall outside 5.4% of 226 pm. This also proves that the tetragonal stabilization of ZrO_2 is dependent on the average radius of tetragonal ZrO_2, 226 pm, and not of the exact radius of 206 pm and 246 pm. At 800 °C tetragonal ZrO_2 could be expected to have high vibrational amplitudes and to be disordered. It is therefore inappropriate to assume that the bond lengths would be identical to those at ambient temperatures and it is even possible that the bond lengths at these temperatures could be 226 pm long.

4. Conclusion

Evidence was obtained that *c*-type rare earth M_2O_3 stabilized ZrO_2 in the tetragonal phase via oxygen coordination between the M_2O_3 molecule and the ZrO_2 unit cell. The ratio for 100% stabilization was calculated to be 2.7 mol% M_2O_3 stabilizer. This was experimentally proved by using the co-decomposition process to obtain 100% tetragonal stabilization efficiency. It has also been established that stabilization is dependent on the average Zr–O bond length of 226 pm and not of the exact radii of 206 pm and 246 pm.

Furthermore it was also proved that the optimum stabilization efficiency is due to co-decomposition and not to a co-precipitated intermediate as was incorrectly assumed. This process is of great importance to the ceramic industry because of the cost savings of ytrria [12] to obtain 100% tetragonal stabilization efficiency. CeO_2 also stabilized ZrO_2 in a tetragonal phase and the mechanism for MO_2 stabilizers as well as the mechanism for cubic stabilization will be researched.

Acknowledgements

The author would like to express his most sincere gratitude to Prof A. Heyns, Dr C. A. Strydom and Mrs S. Verryn for their assistance and guidance.

References

1. F. F. LANGE, *J. Mater. Sci.* **17** (1982) 225.
2. P. H. RIETH, J. S. REED and A. W. NAUMANN, *Bull. Am. Ceram. Soc.* **55** (1976) 717.
3. T. K. GUPTA, *Science of Sintering* **10** (1978) 205.
4. T. K. GUPTA, F. F. LANGE and J. H. BECHTOLD, *J. Mater. Sci.* **13** (1978) 1464.
5. T. K. GUPTA, J. H. BECHTOLD, R. C. KUZNICKIE, L. H. CADOFF and B. R. ROSSING, *J. Mat. Sci* **12** (1977) 2421.
6. M. A. C. G. VAN DE GRAFF and A. J. BURGGRAAF, in Advances in Ceramics, Science and Technology of 'zirconia II, edited by N. Claussen, M. Rihle and A. M. Heuer. (Amer. Ceram. Soc., Ohio, 1984) **12**, p. 744.
7. C. A. STRYDOM and G. PRETORIUS, *Thermochim. Acta*, **223** (1993) 223.
8. W. M. KRIVEN, *J. Mat. Sci. Eng.* **A127** (1990) 249.
9. R. P. INGEL and D. LEWIS, *J. Am. Ceram. Soc.* **64** (1986) 325.
10. R. D. SHANNON, *Acta Crystallogr.* **A32** (1976) 751.
11. G. TEUFER, *Acta Crystallogr.* **15** (1962) 1187.
12. G. PRETORIUS, SA Patent Application No. 92/7315, 1992, South Africa.

Received 21 December 1993
and accepted 27 July1994